Materials Letters 63 (2009) 1019–1022

Contents lists available at ScienceDirect

Materials Letters

journal homepage: www.elsevier.com/locate/matlet

Solvothermally grown ZnO nanorod arrays on (101) and (002) single- and poly-crystalline Zn metal substrates

Je Hyeong Park, P. Muralidharan, Do Kyung Kim *

Department of Materials Science and Engineering, Korea Advanced Institute of Science and Technology (KAIST), 335 Gwahangno, Yuseong-gu, Daejeon 305-701, Republic of Korea

ARTICLE INFO

Article history:
Received 17 November 2008
Accepted 27 January 2009
Available online 5 February 2009

Keywords:
Luminescence
Single-crystal Zn substrate
Solvothermal process
1D ZnO nanorod
Nanomaterials

ABSTRACT

One-dimensional (1D) ZnO nanorod (NR) arrays were grown on (101) and (002) single- and poly-crystalline Zn substrates via direct surface-oxidation in solution, i.e. solvothermal method. The surface-oxidation was done in a solvent mixture of water and 1-propanol with the optimum pH adjusted by adding ammonia. X-ray diffraction patterns revealed that the ZnO NRs grown on the Zn substrates were of single-crystalline with wurtzite structure. The ZnO NRs grown on the (002) single- and poly-crystalline substrates grew in the <001> direction, in contrast to the NRs grown on the (101) single-crystal substrate which were oriented predominantly in the <101> direction. The texture coefficient of the grown ZnO NRs was calculated from the XRD data. Well-aligned NRs that had tips of various shapes were examined by scanning electron microscopy and transmission electron microscopy techniques. The optical properties of the ZnO NRs grown on the Zn substrates were characterized by photoluminescence (PL) spectroscopy.

1. Introduction

One-dimensional (1D) zinc oxide (ZnO) nanostructures (wires, rods, tubes, ribbons, and fibers) have become the focus of research interest due to their wide-band gap (3.37 eV), large free exciton binding energy of 60 meV, high optical gain, and their chemical and thermal stabilities [1–3]. In particular, well-aligned 1D ZnO nanorods/nanowires with novel excitonic properties fabricated on specific substrates have attracted considerable interest for many potential applications in optoelectronic nanoscale devices, including gas sensors, antistatic coatings, optical waveguides, and dye-sensitized solar cells [3–7].

Single-crystalline ZnO nanostructures with various sizes, morphologies, defects and impurities have been synthesized by various methods [8–10], including solvo- and hydrothermal processes [11–17]. These processes offer significant advantages, such as chemical homogeneity, low-temperature and high pressure that are required to increase the solubility of the solid precursors. In general, the growth of ZnO nanostructures under the hydrothermal conditions has typically involved substrate coated with nanosized ZnO seeds. In addition, gold (Au), tin (Sn) and platinum (Pt) films having been pre-coated on the growth surface are also used as catalysts. To obtain NRs oriented in a specific direction, the epitaxial orientation relationship between the NRs and the substrate is one of the important factors [13–17].

ZnO NRs aligned in a specific direction have been grown by the direct surface-oxidation of the zinc substrate in a mixture of water and 1-propanol. There is a possibility that large scale synthesis of well-aligned ZnO NR arrays can be achieved by this method at low-temperature.

In the present work, we demonstrate the fabrication of well-aligned 1D ZnO NRs arrays grown on (101) and (002) single- and poly-crystalline Zn substrates with different tip shape morphologies via a solvothermal process without any metal catalysts. To the best of our knowledge, this is the first report on the effects of single-crystal Zn metal as a source for the growth of the ZnO NRs in a specific crystalline orientation.

2. Experimental

Well-aligned 1D ZnO NR arrays were grown on the (101) and (002) single- (Mateck, Germany) and poly-crystalline zinc sheets (Samhwa, Korea). The zinc sheets acted as both a zinc precursor and a substrate and were initially pretreated by sonication in *iso*-propanol, methanol, and dried in nitrogen gas. The cleaned zinc sheets were placed at the bottom of the 100 mL Teflon-lined stainless steel autoclave containing a mixture of 20 mL of deionized water, and 40 mL of 1-propanol (99.5%, Junsei Chemical, Japan) as a solvent medium. The pH value of the medium was adjusted to an optimum one by adding ammonia (28 wt.%). The solvothermal reaction was conducted in an oven at 125 °C for 10 h. After that, the samples were taken out and rinsed with deionized water and ethanol.

The as-prepared products on the substrates were characterized by an X-ray diffractometer (XRD, Rigaku, D/MAX-IIIC X-ray diffractometer, Tokyo, Japan) with Cu Kα radiation (λ = 0.15406 nm at 40 kV and 45 mA). The growth of ZnO crystallites on the single- and poly-crystalline Zn substrates were quantitatively characterized and

* Corresponding author. Tel.: +82 42 350 4118; fax: +82 42 350 3310.
E-mail address: dkkim@kaist.ac.kr (D.K. Kim).

0167-577X/$ – see front matter © 2009 Elsevier B.V. All rights reserved.
doi:10.1016/j.matlet.2009.01.076

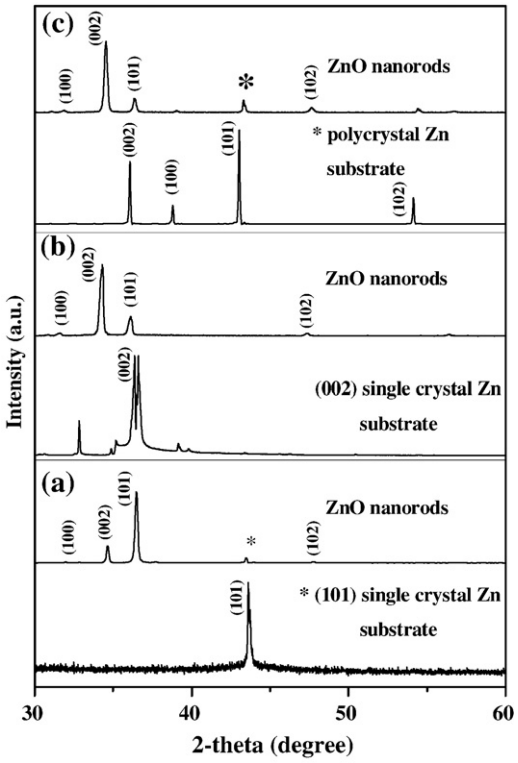

Fig. 1. XRD patterns of the Zn substrates and 1D ZnO NRs grown on (a) (101), (b) (002) single- and (c) poly-crystalline Zn substrates.

compared with calculated texture coefficient $T_{c(hkl)}$. The texture coefficient $T_{c(hkl)}$ is defined as follows [18]: $T_{c(hkl)} = (I_{(hkl)}/I_{r(hkl)})/[1/n\Sigma(I_{(hkl)}/I_{r(hkl)})]$, where $T_{c(hkl)}$ is the texture coefficient, n is the number of peaks considered, $I_{(hkl)}$ are the intensities of the peaks of the ZnO NRs, and $I_{r(hkl)}$ are the peak intensities indicated in the JCPDS #36-1451 corresponding to the randomly oriented crystallites. A sample with randomly oriented crystallites presents a $T_{c(hkl)}$ of 1, while a larger value indicates an abundance of crystallites oriented to the (*hkl*) plane. Field emission scanning electron microscopy (FE-SEM, XL30, FEG, Philips, Netherlands) and transmission electron microscopy (TEM, JEM 3010, JEOL, Japan) were employed to characterize the morphology and structure of the prepared samples. The optical properties of the NRs were characterized at room temperature by photoluminescence (PL) spectroscopy using the 325 nm excitation wavelength from an argon ion laser (Coherent Innova Laser System).

3. Results and discussion

A pale gray ZnO layer grew on the surface of the (101), (002) single- and poly-crystalline zinc substrates by way of a solvothermal reaction at 125 °C for 10 h. The XRD patterns of the ZnO NRs that were grown on the (101) and (002) single- and poly-crystalline zinc substrates together with those of the substrates are shown in Fig. 1(a)–(c). The diffraction peaks of the ZnO NRs are indexed in a hexagonal wurtzite structure ZnO (space group $P6_3mc$), which agrees well with the reported values of lattice constants ($a = 0.324$ nm, and $c = 0.520$ nm) of zincite of the JCPDS # 36-1451.

The orientation of the substrates and the calculated texture coefficient of the ZnO NRs are presented in Table 1. The experiment was repeated for reproducibility and uniformity. The orientation of the single-crystal substrates plays a vital role in determining the preferential growth direction of ZnO crystals. The relative intensities of the major peaks of the ZnO crystals in Fig. 1(a)–(c) were found to be different from one another. This is because their growth orientation depends on the crystallinity and orientations of the substrates. The XRD patterns in Fig. 1(a)–(c) show that the peaks corresponding to the substrates have very weak intensity indicating that the crystalline NRs were grown densely. It can be seen in Fig. 1(a) that the intensity of the (101) peak is strong in comparison with that of the other peaks, such as (002) and (100). This indicates that the ZnO NRs grown on (101) Zn substrate were highly oriented in the <101> direction. The XRD analysis and texture coefficient calculation revealed that the (101) orientation with a high texture coefficient $T_{c(101)}$ is stronger than the (002) orientation with $T_{c(002)}$ (Table 1). The results confirmed that the ZnO NRs grown on the (101) single-crystal Zn substrate were oriented in the <101> direction. On the other hand, NRs grown on the (002) single- and poly-crystalline Zn substrates in Fig. 1 (b) and (c) show that the intensity of the (002) peak is stronger than that of the (101) and (100) peaks. It is evident from the XRD patterns in Fig. 1(b) and (c) that the ZnO crystal was oriented in the <001> direction, as seen quantitatively from the high texture coefficient of $T_{c(002)}$ in comparison with $T_{c(101)}$ (Table 1).

Several reports have revealed that the ZnO NRs grown on the substrates were oriented in the <001> direction because the (001) plane (terminated with zinc) of ZnO has the maximum surface energy, while the (00-1) plane (terminated with oxygen) has the minimum surface energy. As a result, the growth along the <001> direction has a faster rate than that along other directions. The orientation is also determined by surface diffusion and in addition, surface diffusion promotes both *c*-axis and *a*-axis orientations [19]. It is widely recognized that during first growth, interaction between substrate and particles arriving there, play an important role in nucleation. After an initial layer covering the substrate has formed, actual growth begins, during which interaction only occurs between particles of the initial layer. This is true even for amorphous glass substrates, where no epitaxial growth is expected [20,21]. Therefore, it can be concluded in the present study that the ZnO crystallites grow in a specific direction depending on the formation initial nuclei through surface diffusion on the metallic Zn substrate.

Fig. 2(a), (c), (e) and (f) shows the SEM micrographs of densely grown ZnO NRs on the (101), (002) single- and poly-crystalline Zn substrates. The micrographs in Fig. 2(a), (c), (e) and (f) show that the aligned ZnO NRs are oriented perpendicular to the substrate. These ZnO NRs have the same averaged height (~4–5 μm) and diameters (~200 nm). By changing the reaction time period the height of the ZnO NRs could be varied from several hundred nm to several μm. Fig. 2 (b) and (d) shows the SEM and inset TEM images of sharp or prismatic and flat tip shapes of ZnO NRs grown from the (101) and (002) single-crystals, respectively. Fig. 2(f) shows the side-view of the aligned ZnO NRs grown on the poly-crystalline Zn substrate and also the clear tip shape of the NRs.

ZnO NRs grown on the Zn substrates in a basic medium of water/1-proponol under a high pressure may be simplified as follows: $Zn^{2+} + 4OH^- \rightarrow [Zn(OH)_4]^{2-}$ and $[Zn(OH)_4]^{2-} \rightarrow ZnO + H_2O + 2OH^-$. This ensures the dissolution of the Zn^{2+} ion from the metal surface and complexes causing it to form $Zn(OH)_2$ and with the excess OH^- ions to produce $[Zn(OH)_4]^{2-}$ ions. These $Zn(OH)_2$ and $[Zn(OH)_4]^{2-}$ transforms to a ZnO seed at high temperature and pressure. These seeds agglomerate together to form a hexagonal planar nucleus [22]. One face of the hexagonal sheet is Zn rich of ZnO and forms (001)

Table 1
Orientation of the Zn substrates and texture coefficient [$T_{c(hkl)}$] of the grown ZnO NRs at 125 °C

Orientation of the Zn substrate	Texture coefficient	
	$T_{c(002)}$	$T_{c(101)}$
(101)	1.3	2.5
(002)	1.5	0.4
Poly-crystal	1.4	0.4

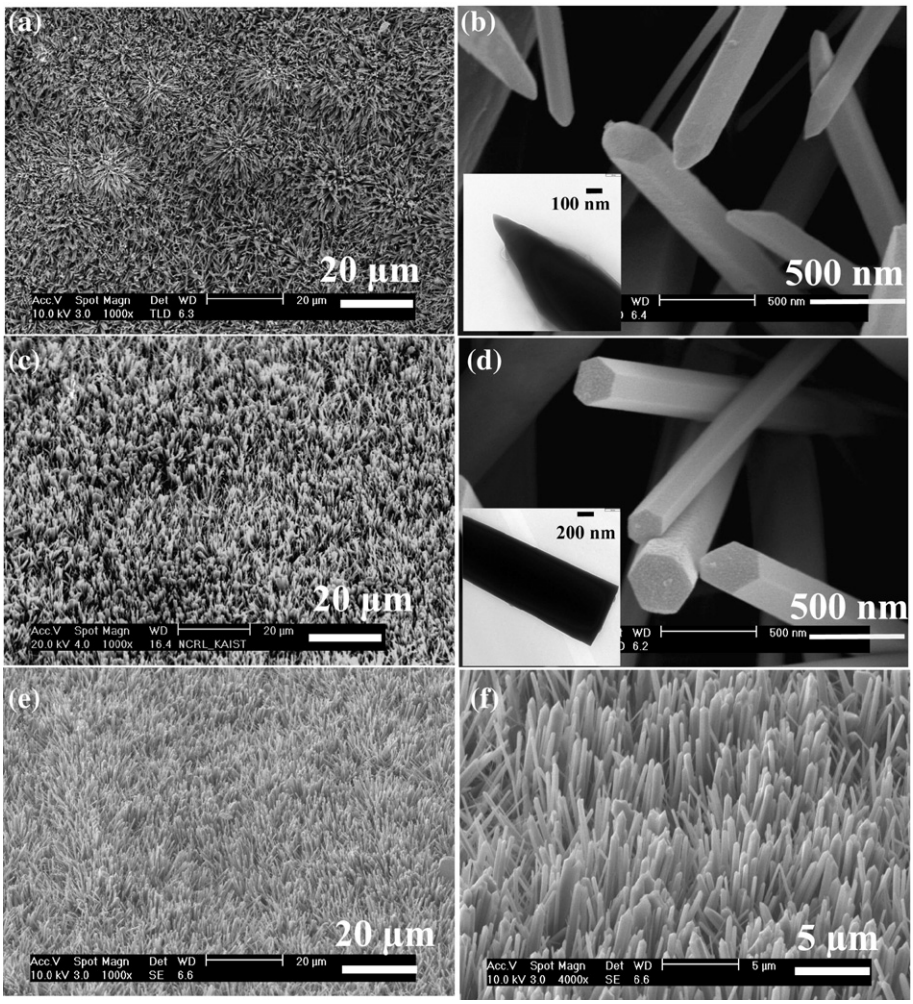

Fig. 2. SEM micrographs of the 1D ZnO NRs grown on (a) (101), (c) (002) single-, and (e) poly-crystalline Zn substrates and high magnification SEM, and inset TEM images of the ZnO NRs grown from (b) (101) and (d) (002) single-crystals and (f) side-view of the ZnO NRs grown on the poly-crystalline Zn substrates.

orientation and can attract new ZnO species to the surface and thereby originate growth. The present experimental results demonstrate the entire Zn^{2+} ion nuclei originated via the dissolution of (101) and (002) orientations of Zn substrates. As a result, it can be concluded that Zn^{2+} ion nuclei originated from different orientations of the substrates and that those seeds agglomerate together to form a hexagonal planar nucleus on the orientation corresponding to the formation of the ZnO crystals. Further experiments are under way to challenge this study, and to improve particle organization and orientation.

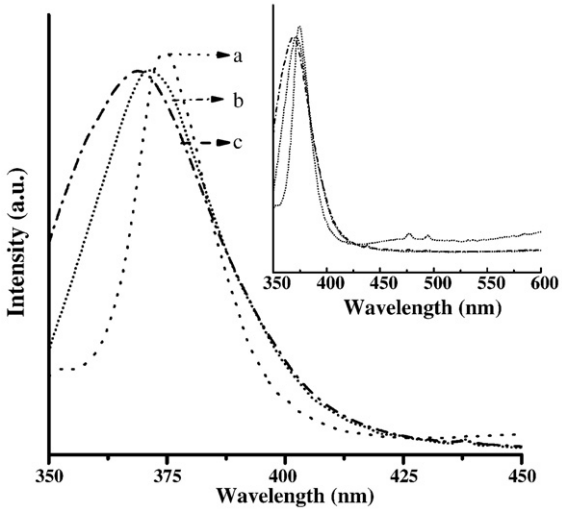

Fig. 3. PL spectra for the 1D ZnO NRs grown on the (a) (101), (b) (002) single- and (c) polycrystalline Zn substrates. The inset shows the PL spectra of entire ranges from 350 to 600 nm.

Fig. 3 shows the PL spectra of the aligned ZnO NRs grown on the Zn substrates, measured in the range of 350 nm to 450 nm, with the inset showing the entire range from 350 to 600 nm. The intense PL peaks centered at ~374 (3.31 eV), 372 (3.32 eV) and 368 (3.36 eV) for the ZnO NRs grown on the (101), (002) single- and poly-crystalline substrates, respectively. The broad UV emission peak range from 368 to 376 nm may correspond to the band edge emission resulting from the recombination of the free excitonic centers [23]. In Fig. 3(b) and (c), the FWHM values of the PL spectra are extremely large and PL peak energies of the NRs grown on the (002) single- and poly-crystalline are higher than the calculated free-exciton energy. The higher PL energies may be attributed to additional UV emission possibly arises from the interface layer between the substrate and the ZnO NRs. In particular, ZnO NRs grown on (101) show very weak peaks at 477 nm and 490 nm. This may be attributed to weak blue bands.

4. Conclusion

The 1D ZnO NRs were successfully grown on (101), (002) single- and poly-crystalline Zn substrates in a basic medium of water/1-proponol via the solvothermal process. The reaction process was

achieved via the simple surface-oxidation of the Zn substrates and the ZnO NRs were grown without any surface catalyst. ZnO NRs that were aligned along the specific orientation were grown with various tip shapes by simply altering the Zn substrates orientations. Thus synthesized aligned ZnO NRs can be directly used for the specific applications, including UV lasers, piezoelectric antenna arrays and field emission devices.

Acknowledgements

This work was supported by the Center for Advanced Materials Processing (CAMP) of the 21st Century Frontier R&D program funded by the MOST and Brain Korea 21 program from Korean Ministry of Education. PM thanks to the Korea Research Foundation Grant funded by the Korean government (MOEHRD) (KRF-2005-005-J09701).

References

[1] Ng HT, Li J, Smith MK, Nguyen P, Cassell A, Han J, et al. Science 2003;300:1249.
[2] Guo L, Ji YL, Xu H, Simon P, Wu Z. J Am Chem Soc 2002;124:14864–5.
[3] Wang ZL, Song J. Science 2006;312:242–6.
[4] Yan H, He R, Pham J, Yang P. Adv Mater 2003;15:402–5.
[5] Wang X, Summers CJ, Wang ZL. Nano Lett 2004;4:423–6.
[6] Cheng C, Xu G, Zhang H, Luo Y, Li Y. Mater Lett 2008;62:3733–5.
[7] Hamann TW, Martinson ABF, Elam JW, Pellin MJ, Hupp JT. Adv Mater 2008;20:1560–4.
[8] Xing GZ, Yi JB, Tao JG, Liu T, Wong LM, Zhang Z, et al. Adv Mater 2008;20:3521–7.
[9] Xu C, Rho K, Chun J, Kim DE. Appl Phys Lett 2005;87 253104-1-3.
[10] Manzoor U, Kim DK. Scripta Mater 2006;54:807–11.
[11] Polsongkrama D, Chamninok P, Pukird S, Chow L, Lupan O, Chai G, et al. Physica B 2008;403:3713–7.
[12] Wang Z, Huang B, Liu X, Qin X, Zhang X, Wei J, et al. Mater Lett 2008;62:2637–9.
[13] Wang J, Sha J, Yang Q, Ma X, Zhnag H, Yu J, et al. Mater Lett 2005;59:2710–4.
[14] Vayssieres L. Adv Mater 2003;15:464–6.
[15] Movahedi M, Kowsari E, Mahjoub AR, Yavari I. Mater Lett 2008;62:3856–8.
[16] Le HQ, Chua SJ, Koh YW, Loh KP, Fitzgerald EA. J Cryst Growth 2006;293:36–42.
[17] Wang JX, Sun XW, Yang Y, Huang H, Lee YC, Tan OK, et al. Nanotech 2006;17:4995–8.
[18] Romero R, Leinen D, Dalchiele EA, Ramos-Barrado JR, Martín F. Thin Solid Films 2006;515:1942–9.
[19] Kajikawa Y. J Cryst Growth 2006;289:387–94.
[20] Znaidi L, Soler Illia GJAA, Benyahia S, Sanchez C, Kanaev AV. Thin Solid Films 2003;428:257–62.
[21] Hong J, Helming H, Jiang X, Szyszka B. Appl Surf Sci 2004;226:378–86.
[22] Li W-J, Shi E-W, Zhong W-Z, Yin Z-W. J Cryst Growth 1999;203:186–96.
[23] Huang MH, Wu Y, Feick H, Tran N, Weber E, Yang P. Adv Mater 2001;13:113–6.